

## Shock waves and time scales to reach equipartition in the Fermi-Pasta-Ulam model

Pietro Poggi,<sup>1</sup> Stefano Ruffo,<sup>2,\*</sup> and Holger Kantz<sup>3</sup><sup>1</sup>Centre E. Borel, Institut Henri Poincaré, 11 Rue Pierre et Marie Curie, 75231 Paris, France<sup>2</sup>Dipartimento di Energetica, Università di Firenze, Via S. Marta 3, Firenze, Italy, and INFN Sezione di Firenze and INFN, Unità di Firenze, Firenze, Italy<sup>3</sup>Max-Planck-Institut für Physik Komplexer Systeme, Bayreuther Strasse 40, Haus 16, D-01187 Dresden, Germany

(Received 16 January 1995)

In a specific continuum limit at intermediate energy, the Fermi-Pasta-Ulam (FPU)- $\beta$  chain can be described by a nonlinear partial differential equation, whose solutions are shock waves. Proper long-wavelength initial conditions of the discrete model show a time evolution in numerical simulations that agrees with the solution of the continuum model where it is single valued. The breakdown times for the occurrence of the shock, when starting from a smooth initial condition, are shown to be relevant time scales for the transition to equipartition of energy, by an analysis of the time evolution of the spectral entropy. A simple time scale  $t_B \sim N^2/(\beta kE)$  is derived in the continuum limit for mode  $k$  initial excitations with energy  $E$  and  $N$  particles. This time scale is tested numerically in the FPU chain.

PACS number(s): 05.45.+b, 63.20.Ry, 63.10.+a

## I. INTRODUCTION

The FPU  $\beta$  model [1], given by the Hamiltonian

$$H = \sum_{n=1}^N \left( \frac{p_n^2}{2} + \frac{(q_{n+1} - q_n)^2}{2} + \beta \frac{(q_{n+1} - q_n)^4}{4} \right) \quad (1)$$

with periodic boundary conditions  $q_1 = q_{N+1}$ ,  $p_1 = p_{N+1}$ , is a paradigm for a nonintegrable Hamiltonian system with many degrees of freedom and has a simple integrable limit (harmonic chain). In this limit, the solutions are Fourier modes with wave numbers  $2\pi k/N$  and frequencies  $\omega_k = 2 \sin(\pi k/N)$ , where  $N$  is the number of particles in the chain and  $|k| = 1, \dots, N/2$ . One issue of many studies is the equipartition of energy when leaving the harmonic limit, i.e., the redistribution of energy among the different modes. The *spectral entropy* [2] proved to be a useful probe for the observation of equipartition. When defining “probabilities”  $p_k(t) = E_k(t)/\sum_l E_l$ , where  $E_k(t) = (P_k^2 + \omega_k^2 Q_k^2)/2$  is the actual energy of the  $k$ th Fourier mode [determined from the amplitudes  $\{Q_k(t)\}$  and  $\{P_k(t)\}$  of the Fourier transform of  $\{q_n(t)\}$  and  $\{p_n(t)\}$ ], the spectral entropy reads  $S(t) = -\sum_k p_k \ln p_k$ , following Shannon. In the case where only a single Fourier mode is excited,  $S$  assumes the value 0, whereas in an equilibrium situation (i.e., equipartition)  $S = S_{\max} = \ln(N/2)$ . When varying the number of degrees of freedom  $N$  or the type of initial condition the normalized order parameter  $\eta(t) = [S(t) - S_{\max}]/[S(0) - S_{\max}]$  is more useful [2].

There exist various regimes in energy, characterized

by different relaxation times to equipartition; they have been recently described in Refs. [3,4]. Below a critical energy ( $E_c \approx 3$  for  $\beta = 0.1$ ), no significant diffusion to high modes from the initially excited low modes is observed [5]. This is the region where perturbation theory estimates in the manner of Nekhoroshev have been recently attempted (they are reviewed in Ref. [6]). This is also the region of FPU recurrences of individual mode energies [7], which have also been explained in terms of a continuum model for the cubic FPU  $\alpha$  model [8,9], the Korteweg-deVries equation. The quasiperiodic behavior is believed to be the consequence of the presence of “solitons,” which travel on the lattice and almost reproduce the initial condition at given instants of time. Above  $E_c$  the system relaxes to equipartition on times which grow with  $N$  [5,10] and recurrent behaviors disappear, rendering meaningless the soliton interpretation. At even larger energies  $E \sim N$  mode resonance overlap [11] causes a fast relaxation to equipartition, detected also in some other early numerical experiments [12]; this also reflects in a change in the scaling law of the maximal Lyapunov exponent vs energy density [13], which has been recently analytically computed using differential geometry techniques [14].

In this paper we concentrate on the energy region  $E_c < E < O(N)$ , where the FPU chain evolves towards equipartition on a long time scale. We study the propagation of traveling waves with wavelength of the order of the system size ( $N$ ), focusing on the mechanism by which the nonintegrability of the system causes the destruction of such structures. This will give us information about the times for relaxation to equipartition, measured using the parameter  $\eta$ , for energies larger than the equipartition threshold. As we are treating one-mode excitations we have

$$\eta(t) = 1 - \frac{S(t)}{S_{\max}}. \quad (2)$$

\*Also at Laboratoire de Physique Quantique, Université Paul Sabatier, and URA 505, CNRS, Toulouse, France.

In Sec. II we present the derivation of the PDE corresponding to the continuum limit of model (1) for sufficiently large energy. The PDE, which develops shocks, is then solved in Sec. III and the relevant dependences of the breakdown time are given, e.g., that on the number of oscillators  $N$  and on the strength of the nonlinearity. Section IV is devoted to the comparison between the continuum model and the numerical solution of the FPU lattice. At the breakdown time energy transfer to short wavelengths is enhanced through a dynamical mechanism which creates short scale oscillations where the slope of the solution is larger; then the breakdown time is assumed as a typical time scale for the initial evolution towards equipartition and the spectral entropy time dependence is rescaled accordingly. Numerical experiments show a good agreement with this theory. In Sec. V we draw some conclusions and compare our results with those obtained with different initial and boundary conditions.

## II. THE CONTINUUM LIMIT

For sufficiently smooth initial conditions, the time evolution of system (1) can be understood in terms of an appropriate continuum limit. We must, however, observe that the limiting process from a discrete system to a continuous one, as the inverse process of discretization, is not uniquely defined and can introduce some new qualitative properties, depending on the employed procedure. Nevertheless, one can at least hope to sketch some analogies, whose validity can be checked by numerical experiments.

The equations of motion for the FPU  $\beta$  system are

$$\ddot{q}_n = q_{n+1} - 2q_n + q_{n-1} + \beta(q_{n+1} - q_n)^3 - \beta(q_n - q_{n-1})^3. \quad (3)$$

We consider an initial configuration which is characterized by a slow variation of the coordinate  $q_n$  of the  $n$ th particle with respect to the lattice site  $n$ , such as a single linear mode with a small  $k$ :

$$q_n(0) = A \cos\left(\frac{2\pi kn}{N}\right), \quad n = 1, \dots, N; \quad k \ll N. \quad (4)$$

In the continuum approach we consider the set of coordinates  $\{q_n(t)\}$  as a sampling, at fixed integer positions, of a field  $q(x, t)$  defined on a continuous spatial domain:

$$q_n(t) = q(x = n, t). \quad (5)$$

The field  $q(x, t)$  must obey the boundary conditions which correspond to those of the lattice: for periodic boundary conditions we can consider the whole real line as the spatial domain of  $q(x, t)$ , imposing the periodicity condition  $q(x + N, t) = q(x, t)$ . We suppose that  $q(x, 0)$  is slowly varying over spatial distances of the order of  $\Delta x \approx 1$  (the lattice spacing), i.e., the waveform varies significantly only over a characteristic distance of size  $N$ ; this condition will remain true at least for some initial short time interval. During this time interval the evolution of the field can thus be described by substituting a

suitably truncated Taylor expansion to the finite differences on the right-hand side of (3).

Let us first consider the linear term to clarify in which parameter the expansion has to be made. By the substitution

$$[q_{n+1}(t) - 2q_n(t) + q_{n-1}(t)] \longrightarrow [q(x+1, t) - 2q(x, t) + q(x-1, t)],$$

we observe that using the shift operator  $\exp[\Delta x \partial/\partial x]$  with increment  $\Delta x = 1$  we can write

$$\begin{aligned} [q(x+1, t) - 2q(x, t) + q(x-1, t)] \\ &= 2 \left[ \cosh\left(\frac{\partial}{\partial x}\right) - 1 \right] q(x, t) \\ &= \frac{\partial^2}{\partial x^2} q(x, t) + \frac{1}{12} \frac{\partial^4}{\partial x^4} q(x, t) + \dots \end{aligned} \quad (6)$$

If  $q(x, 0) = A \cos(2\pi kx/N)$  then the order of magnitude of the different terms in this expansion is determined by  $|\partial q/\partial x| \approx |kA/N| \approx |A/N|$  (for  $k \ll N$ ). Therefore, the expansion in increasing order of derivatives is an expansion in powers of  $k/N = O(1/N)$ . In other words the small parameter whose powers enter in the expansion is the wave number, which in our units is  $2\pi k/N$ . Thus, expansion (6) is equivalent to an expansion of the dispersion law near the nondispersive limit  $k \rightarrow 0$ , which is in fact valid for long waves. The development on the right-hand side of (6) takes into account the discreteness of the medium, which causes dispersion. Retaining only the first term would lead, in the linear case, to the usual vibrating string equation. Let us now define

$$\tilde{x} = \frac{x}{N}, \quad (7)$$

$$\tilde{t} = \frac{t}{N}, \quad (8)$$

$$\tilde{q}(\tilde{x}, \tilde{t}) = \frac{q(x, t)}{A}. \quad (9)$$

The normalizations (7) and (9) make the order of the terms explicit;  $\tilde{q}$  and its spatial derivatives  $\partial^j \tilde{q}/\partial \tilde{x}^j$  are of the order 1, and the order of magnitude is explicitly given by the coefficients. We also observe that in these variables the basic periodicity interval for  $\tilde{q}(\tilde{x}, \tilde{t})$  is always  $\tilde{x} \in [0, 1]$ , irrespective of  $N$ , so for a given  $k$  the continuum approximation is increasingly more accurate as we increase  $N$ . Finally, transformation (8) normalizes the time scale to the period of the slowest linear mode which is of order  $N$ . Equation (6) yields

$$\begin{aligned} q(x+1, t) - 2q(x, t) + q(x-1, t) \\ &= A \left[ \frac{1}{N^2} \frac{\partial^2 \tilde{q}}{\partial \tilde{x}^2} + \frac{1}{12N^4} \frac{\partial^4 \tilde{q}}{\partial \tilde{x}^4} + O\left(\frac{1}{N^6}\right) \right], \end{aligned}$$

while for the nonlinear term we obtain

$$\beta[(q_{n+1} - q_n)^3 - (q_n - q_{n-1})^3]$$

$$\rightarrow \beta A^3 \left[ \frac{3}{N^4} \left( \frac{\partial \tilde{q}}{\partial \tilde{x}} \right)^2 \frac{\partial^2 \tilde{q}}{\partial \tilde{x}^2} + O \left( \frac{1}{N^5} \right) \right].$$

Introducing the parameters

$$\delta = \frac{1}{N}, \quad \epsilon = \beta A^2,$$

related to dispersion and to nonlinearity respectively, we finally obtain the evolution equation for  $\tilde{q}(\tilde{x}, \tilde{t})$ :

$$\begin{aligned} \frac{\partial^2 \tilde{q}}{\partial \tilde{t}^2} &= \frac{\partial^2 \tilde{q}}{\partial \tilde{x}^2} + \frac{\delta^2}{12} \frac{\partial^4 \tilde{q}}{\partial \tilde{x}^4} + 3\epsilon\delta^2 \left( \frac{\partial \tilde{q}}{\partial \tilde{x}} \right)^2 \frac{\partial^2 \tilde{q}}{\partial \tilde{x}^2} \\ &+ O(\delta^4) + O(\epsilon\delta^3). \end{aligned} \quad (10)$$

As long as the spatial derivatives of  $\tilde{q}$  remain  $O(1)$  the order of magnitude of the terms is explicitly given by  $\epsilon$  and  $\delta$ . We are interested in studying the evolution starting from an initial condition which, in the linear case ( $\beta = 0$ ), would give rise to a traveling wave running in one direction. In such a case one can expect the solution, at least initially, to be slowly changing in time when observed in a translating reference frame with the linear wave velocity, which is  $\approx 1$  for the low modes. Therefore, choosing for example a right-going wave, we define

$$\tilde{q}(\tilde{x}, \tilde{t}) = \phi(\xi, \tau) \quad (11)$$

with

$$\begin{cases} \xi = \tilde{x} - \tilde{t} \\ \tau = \delta^2 \tilde{t}, \end{cases} \quad (12)$$

where the variable  $\tau$  governs the variation on a slower time scale, corresponding to sizeable modifications of the shape of the traveling wave. Inserting (11) and (12) in Eq. (10) and neglecting terms of order higher than  $\delta^2$ , we obtain the following evolution equation for the function  $w \equiv \partial\phi/\partial\xi$ :

$$w_\tau = -\frac{3}{2}\epsilon w^2 w_\xi - \frac{1}{24} w \xi \xi \xi, \quad (13)$$

where partial derivatives are now denoted by the subscript for convenience in later calculations. Let us observe that the evolution equation (13) is of lower order in time because one of the two possible propagation directions has been selected. Equation (13) is the well known modified Korteweg–deVries equation, an integrable nonlinear field equation solvable by the inverse scattering method (see [15] and references therein). The study of the solutions of this equation allows one to explain qualitatively the recurrences observed numerically in the FPU model at small energy. Let us remember that, for the so-called FPU  $\alpha$  model with cubic nonlinearity in the Hamiltonian, one gets instead the (integrable) Korteweg–deVries equation following an analogous procedure [8]. Equation (13) does not contain any dependence in  $\delta$ , and therefore it is invariant with respect to changes of  $N$ ; in

particular it remains valid in the infinite size  $N \rightarrow \infty$  limit.

### III. SOLUTION OF THE CONTINUUM MODEL

We now consider the case where the nonlinear term prevails over the dispersive one in Eq. (13) yielding

$$w_\tau \simeq -\frac{3}{2}\epsilon w^2 w_\xi, \quad (14)$$

which, rewritten in the variable  $u(x, t) \equiv \partial q(x, t)/\partial x$ , gives

$$u_t + u_x + \frac{3}{2}\beta u^2 u_x = 0. \quad (15)$$

Equation (15) can be solved exactly (in implicit form) by the method of characteristics. To sketch the method we consider the slightly more general case of a nonlinear hyperbolic first order PDE of the quasilinear kind

$$u_t + F(u)u_x = 0. \quad (16)$$

Equations of this form arise in many physical problems [16]. We will now treat briefly Eq. (16) from a general point of view, independently of its connection with the discrete lattice problem, giving a short review of known methods and results.

It can be easily shown that all solutions of (16) have a constant value over a particular family of straight lines in the  $(x, t)$  plane, called characteristic curves. Each of these lines has a slope

$$\frac{dx}{dt} = F(u), \quad (17)$$

where  $u$  is the constant value that  $u(x, t)$  itself takes on the line. The solution of (16) is based on the construction of the family of lines after requiring, in our case, a specific initial condition (a boundary condition is also required if one restricts to a bounded domain). We are interested in the initial value problem

$$u(x, 0) = u_0(x), \quad -\infty < x < \infty. \quad (18)$$

Then  $u$  takes the constant value  $u_0(\zeta)$  on the straight line

$$x = \zeta + F(u_0(\zeta))t, \quad (19)$$

for each value of the parameter  $\zeta$ .

Therefore the solution of the initial value problem (16) and (18) is given in implicit form by

$$\begin{cases} u = u_0(\zeta) \\ x = \zeta + F(u_0(\zeta))t, \end{cases} \quad (20)$$

where  $u(x, t)$  is obtained solving for  $\zeta(x, t)$  in the second equation. The solution (20) means that each different value of  $u$  propagates with its own speed  $F(u)$ ; the waveform changes necessarily in time, being affected by

distortion due to nonlinearity (this distortion vanishes in the linear case).

The most striking phenomenon is the birth of discontinuous solutions, even from smooth initial data. In fact, since the characteristics are not parallel to each other, for  $t > 0$  some of them can intersect. But characteristics with different slopes carry different values of the solution, so an intersection implies a multiple definition of the  $u$  value at that point in the  $(x, t)$  plane. The onset of this is called a shock. In general, there is a region in the  $(x, t)$  plane, bounded by an envelope which depends on the initial waveform, where the characteristics intersect and the solution constructed by propagation over the characteristics is multivalued. This envelope is also, for  $t > 0$ , the boundary of the region on the  $(x, t)$  plane where the solution of (16) exists and is single valued. The instant  $t = t_B$  [see Fig. 1(b)] where the shock arises is the minimum value of  $t$  for the points of the envelope in the  $(x, t)$  plane. To construct the waveform at time  $t$  one has to translate to the right every value  $u_0$  of the initial profile

by a distance  $F(u_0)t$ . Each part of the wave where the propagation speed is decreasing with increasing  $x$  ultimately “breaks” into a multivalued waveform, because points of the waveform with a smaller  $x$  value tend to overtake those with a bigger  $x$  value.

We refer now again to (15), which is of the kind (16) with  $F(u) = 1 + 3\beta u^2/2$ , so the propagation velocity is larger the larger  $|u_0|$  is. The parts of the wave where the nonlinear distortion during propagation causes an increase in slope, leading to shock formation, are those where  $|u_0(\zeta)|$  decreases with increasing  $\zeta$ . In our case the discontinuity always arises because we consider periodic boundary conditions, which implies that it always exists an interval over which  $|u_0(\zeta)|$  is decreasing (apart from the trivial case  $u \equiv 0$ ). An example of a solution of (15), shown in the moving frame, is reported in Fig. 1(a), together with the related characteristics [Fig. 1(b)].

The breakdown time  $t_B$  can be calculated analytically from the solution (20) to be

$$t_B = \left[ \max_{\{\zeta: F'(u_0(\zeta))u'_0(\zeta) < 0\}} |F'(u_0(\zeta))u'_0(\zeta)| \right]^{-1}, \quad (21)$$

giving for (15)

$$t_B = \left[ \max_{\{\zeta: du_0^2(\zeta)/d\zeta < 0\}} |3\beta u_0(\zeta)u'_0(\zeta)| \right]^{-1}. \quad (22)$$

When  $q(x, 0) = A \cos(2\pi kx/N)$ , then

$$u_0(\zeta) = -(2\pi k/N)A \sin(2\pi k\zeta/N), \quad (23)$$

and one obtains

$$t_B = \frac{N^3}{12\pi^3 k^3 \beta A^2}, \quad (24)$$

while the number of space intervals of the waveform where the discontinuity develops is  $2k$  in the interval of length  $N$ .

#### IV. SHOCK WAVES ON THE LATTICE

We have so far discussed the properties of the solutions of Eq. (15). Now we come back to the original problem, the nonlinear chain described by (3), to apply the results of the continuum model, after a suitable interpretation.

The numerical integration of (3) shows that, for appropriate initial conditions which will be specified later, the temporal evolution of the discrete spatial derivative

$$r_n \equiv q_{n+1} - q_n \quad (25)$$

of the lattice configuration  $q_n(t)$  is well described by the solution  $u(x, t)$  of (15), nearly up to the instant  $t = t_B$  at which the latter becomes multivalued (see Fig. 2).

Before entering a detailed analysis let us clarify some aspects of the relation between the discrete lattice described by the equations of motion (3) and the continuum model described by the wave equation (15), reexamining

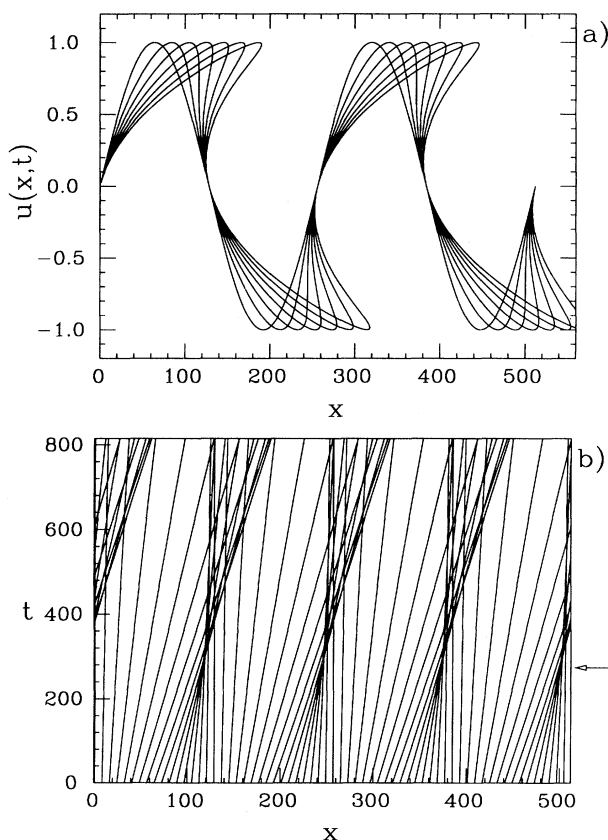


FIG. 1. (a) Solution of Eq. (15) in the moving frame, for the initial condition  $u_0(\zeta) = \sin(2\pi k\zeta/N)$  with  $k = 2$ ,  $N = 512$ , and  $\beta = 0.1$ . The curves are traced stroboscopically from  $t = 0$  to  $t = 3t_B$ , with a time interval of  $t_B/2$  [ $t_B$  being given in (24)]. (b) Diagram of characteristics in the  $(x, t)$  plane. The envelope of characteristics has cusps at  $t = t_B$ , the breakdown time (indicated by the arrow); for  $0 \leq t < t_B$  the solution is single valued.

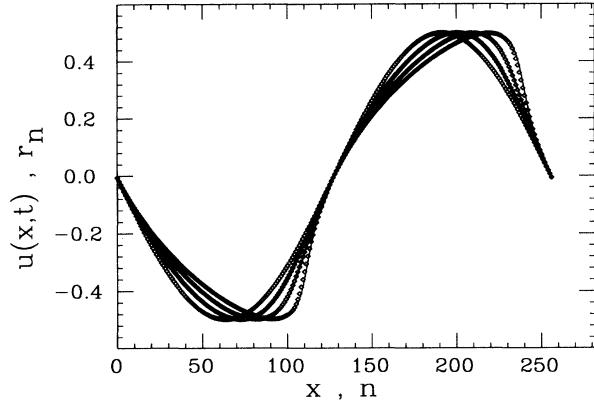


FIG. 2. Comparison of the solution of Eq. (15) (full line) and the solution of the lattice equation (3) ( $\diamond$ ) with the initial condition (27) for  $t < t_B$ . The solution of Eq. (15) is drawn in the moving frame, each time the lattice solution completes a round trip.  $N = 256$ ,  $k = 1$ ,  $R = 4.67 \times 10^{-3}$  [ $R$  is defined in Eq. (28)],  $t_B = 1091$ .

the various hypotheses and approximations which led to the latter. In particular we must specify what kind of initial conditions allows the comparison of  $r_n(t)$  with  $u(x, t)$ . Since the continuum representation is suggested by the hypothesis of a “long wavelength” initial condition, we study the case of an initial excitation restricted to the low modes [i.e., (4)]. The initial conditions to be imposed on (15) involve only  $u(x, 0) = \partial q(x, 0)/\partial x$ . Since Eqs. (3) are of second order, initial velocities remain to be specified. The reduction of (10) to (13) rests on the selection of one of the two possible directions of wave propagation. Then the appropriate initial distribution of velocities on the lattice completing (4) must give rise to a traveling wave. In the linear case the right-going traveling wave corresponding to mode  $k$  is (apart from a constant phase)

$$q_n(t) = A \cos\left(\frac{2\pi kn}{N} - \omega_k t\right), \quad n = 1, \dots, N, \quad (26)$$

which originates from the initial conditions

$$\begin{cases} q_n(0) = A \cos\left(\frac{2\pi kn}{N}\right) \\ \dot{q}_n(0) = \omega_k A \sin\left(\frac{2\pi kn}{N}\right) \end{cases} \quad n = 1, \dots, N, \quad (27)$$

with  $\omega_k = 2 \sin(\pi k/N)$ . It is reasonable to expect that (27) gives rise to a traveling wave, although for  $\beta \neq 0$  its time evolution is not given by (26).

To derive (14), or the equivalent (15), from (13), we have neglected the dispersive term containing  $w_{\xi\xi\xi}$ . It is clear that such a term becomes important where a discontinuity is developing, i.e., when  $t \rightarrow t_B$  and the spatial derivatives increase. Nevertheless, let us point out that (13) is already a truncation of (10). Although the term  $w_{\xi\xi\xi}$  is certainly the most important among the dispersive terms originated from the expansion (6), its relative importance to nonlinear terms, denoted as  $O(\epsilon\delta^3)$

in (10), depends also on  $\epsilon$ , which is not necessarily small. Here we study in fact the regime of sufficiently high energy, in which an initially smooth waveform evolves into a spatially stochastic field. In this case the temporal evolution is not described by the modified Korteweg-deVries equation (13), but by an equation which takes into account nonlinear terms of higher order, which are larger than the dispersion term and destroy integrability. Thus we made the simplest choice of neglecting dispersion while keeping the dominant nonlinear term. Moreover, for  $t > t_B$ , the “smooth wave” hypothesis, on which the continuum approximation is based, is no longer valid.

The energy range of interest is that where a significant energy sharing between the Fourier modes is present. In Ref. [5] it has been found that this happens if  $E > E_c$  ( $E$  is the total energy), with  $E_c \simeq 3$  for  $\beta = 0.1$ , looking at the time evolution of the order parameter  $\eta$  (2), which shows a relaxation towards equipartition. This result is confirmed in Ref. [10], where a theoretical explanation is also given in terms of a diffusion mechanism from low to high modes.

In what follows we report the results of several numerical experiments concerning the integration of the FPU equations of motion (3) starting from initial data of the kind (27) with  $k \ll N$  and with energy density  $E/N$  in the range 0.1–5.8 and  $128 \leq N \leq 1024$ . For lower values of  $E/N$  the system shows recurrent behavior and extremely slow relaxation, while for higher values the breakdown time becomes too short to allow an analysis of the transient behavior. The integration algorithm is the symplectic “leap-frog,” with a temporal step  $\Delta t = 0.05$ , which gives an error in energy conservation less than 0.1%.  $\beta$  was fixed at  $\beta = 0.1$ .

Particularly suitable for this analysis is the use of a “pseudo-Reynolds” number  $R$  as a control parameter [17].  $R$  measures the relative weight of the nonlinearity,

$$R = \frac{E_{nl}}{E_{lin}}, \quad (28)$$

where  $E_{nl}$  is the nonlinear energy of the system (anharmonic potential energy term) at  $t = 0$  while  $E_{lin}$  is the linear energy (kinetic plus the harmonic potential).

The breakdown time dependence on the wave amplitude  $A$ , expressed by (24), can be read as a dependence on the degree of nonlinearity of the system. The latter grows with  $A$ : in the case of one-mode excitations  $R \propto \beta A^2 k^2 / N^2$ , roughly. Indeed, for the initial conditions (27) one can exactly evaluate the quantities in (28) at  $t = 0$ , obtaining

$$E_{lin}(0) = \frac{1}{2} \omega_k^2 N A^2 \quad \xrightarrow{k \ll N} \quad \frac{2\pi^2 k^2 A^2}{N}, \quad (29)$$

$$E_{nl}(0) = \frac{3}{32} \beta \omega_k^4 N A^4 \quad \xrightarrow{k \ll N} \quad \frac{3\pi^4 \beta k^4 A^4}{2N^3}, \quad (30)$$

$$R = \frac{3}{16} \beta \omega_k^2 A^2 \quad \xrightarrow{k \ll N} \quad \frac{3\pi^2 \beta k^2 A^2}{4N^2}, \quad (31)$$

so that

$$R = \frac{3\beta E_{\text{lin}}}{8N}. \quad (32)$$

In the explored energy range, the evolution of the non-linear chain (3), starting from initial conditions of the kind (27), is well described by the continuum model (15) over a time slightly shorter than  $t_B$  (see Fig. 2). The comparison is made between  $r_n(t) = q_{n+1}(t) - q_n(t)$  and  $u(x, t) = \partial q(x, t) / \partial x$  evaluated at lattice points  $x = n$ . This agreement has been verified for different values of  $N$  (from  $N = 64$  to  $N = 512$ ), varying the energy density in the previously given range and for a few values of  $k$  (with  $k \ll N$ ).

As we can see in Fig. 3, the agreement is excellent up to almost  $t = t_B$ . Near this time the  $r_n$  waveform develops short-wavelength oscillations in the shock zone for the wave on the continuum. (For the sake of brevity we will refer to such a zone as the “shock zone” also when we speak about the discrete lattice.)

In order to obtain a quantitative indication how well  $r_n(t)$  represents  $u(x, t)$ , we study the time evolution of the difference between them. In Fig. 4 we show the relative error

$$D\%(t) = \max_{n \in \{1, \dots, N\}} |r_n(t) - u(n, t)| / \max_{n \in \{1, \dots, N\}} |r_n(0)|, \quad (33)$$

as a function of time.

This quantity remains less than a few percent most of the time, then it suddenly increases for times near  $t = t_B$ ; this is mainly due to the shock zone, while the major part of the wave on the lattice remains well approximated by the continuum model (see Figs. 2 and 3). Moreover, we observe that the graph of the multivalued “solution”  $u(x, t)$  for  $t > t_B$  continues to approximate the shape of  $r_n$  away from the shock zone, where  $r_n$  remains smooth for a time of the order of some  $t_B$ 's.

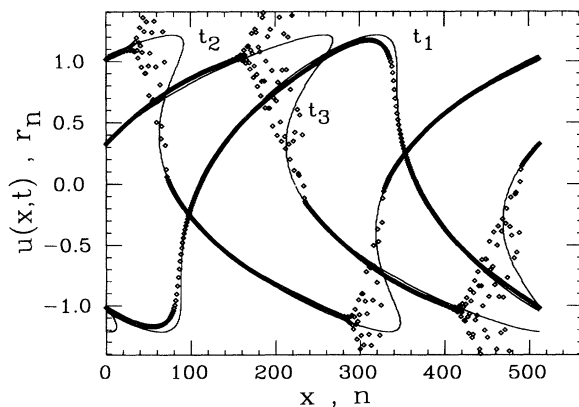


FIG. 3. Comparison between the solution of Eq. (15) (full line) and the solution of the lattice equations of motion (3) ( $\diamond$ ).  $N = 512$ ,  $k = 1$ ,  $R = 2.8 \times 10^{-2}$ ,  $t_B = 364$ . We observe the time evolution in the laboratory frame, where the wave travels to the right. The times  $t_1 = t_B$ ,  $t_2 = 1.6t_B$ , and  $t_3 = 2t_B$  are shown successively.

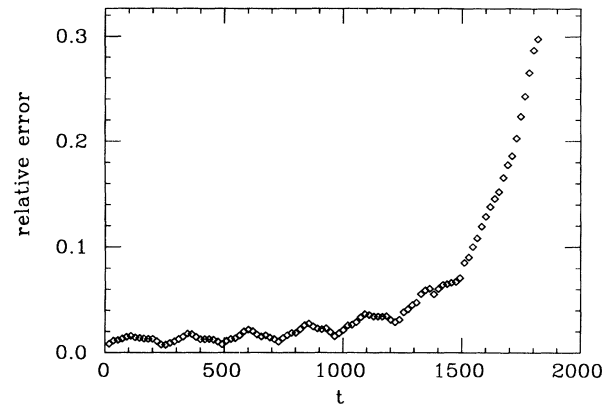


FIG. 4. Relative error of Eq. (33) vs time for  $N = 512$ ,  $k = 1$ ,  $R = 5.6 \times 10^{-3}$ ,  $t_B = 1819$ .

Let us resume our findings. The evolution of the FPU chain can be predicted by the model (15) over times which are relatively small but sufficient for the wave to complete some round trips on the lattice before breaking up. The initially regular waveform, which would remain such if the lattice were linear, becomes more and more irregular as time goes on until it forms a cloud of points without any clear structure. This is shown (at a much larger value of  $R$  to reduce integration times) in Fig. 5, where one can observe the destruction of the wave structure starting from the shock zone where irregular fluctuations are created; the latter then spread, invading the whole chain. In the final state many linear Fourier modes are excited. Thus, for the traveling wave initial conditions considered here, the mechanism causing the redistribution of energy between the modes is a sort of “shock” produced by the nonlinearity of the lattice. Obviously the true shock, described by (15), is a differ-

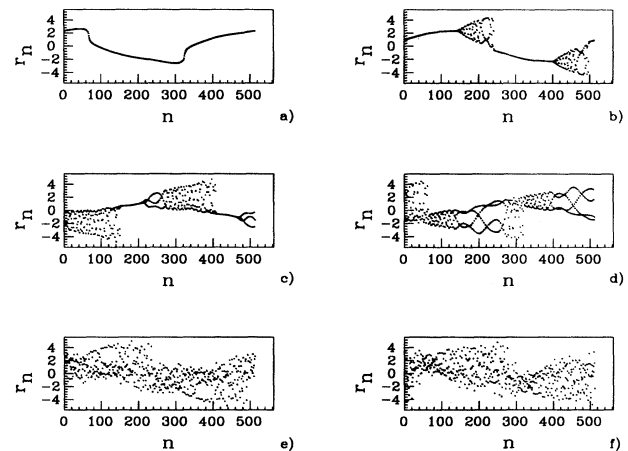


FIG. 5. Time evolution of the discrete spatial derivative  $r_n$  in Eq. (25) vs lattice site  $n$  for longer times: (a)  $t = 90$ , (b)  $t = 210$ , (c)  $t = 330$ , (d)  $t = 450$ , (e)  $t = 570$ , (f)  $t = 600$ . The final waveform displays no regularities.  $N = 512$ ,  $k = 1$ ,  $R = 0.18$ ,  $t_B = 56$ .

ent phenomenon, which nevertheless represents a useful analogy to refer to, and from which quantitative informations can be derived. [To avoid misunderstandings, we emphasize that the solution of (15) exists only until  $t = t_B$ , while the solution of (3) is defined over all times. This is guaranteed by the fact that Newton equations for potentials bounded from below define a flow over all times [18].]

Let us now look at the time evolution of the order parameter  $\eta$  (2). If our interpretation of the shock on the lattice is correct, one must observe an initially slow decrease of  $\eta$ , followed by a sharper decay for  $t > t_B$  corresponding to the energy transfer to small scales caused by the shock. This is indeed what can be seen in Fig. 6, where we have drawn  $\eta(t)$  for one particular value of the nonlinearity parameter  $R$ . Over longer times than those described by our theory,  $\eta$  displays random fluctuations superimposed on a much slower decay (corresponding to the stochastization of the field shown in Fig. 5).

To relate in a quantitative way the evolution of  $\eta$  with the shock wave model, we examine the expression (24) of the breakdown time, when the initial condition is (23), corresponding to (27). Using the parameter  $R$  one gets

$$t_B = \frac{\omega_k^2 N^3}{64\pi^3 k^3 R} \xrightarrow{k \ll N} \frac{N}{16\pi k R}. \quad (34)$$

One can verify that (34) gives the correct order of magnitude for the onset of small scale oscillations in  $r_n$  (see Fig. 3). However, it is not clear how to define and then find a probe for such an onset time. If we consider instead the  $\eta$  evolution we can make more quantitative statements. As shown above, the sharp decay of  $\eta$  is related to the shock on the lattice, so the time scale characterizing this decay of  $\eta$  must be related to the breakdown time. In Fig. 7 the initial behavior of  $\eta$  is drawn for different values of  $R$  showing a more rapid decay as  $R$  is increased. This is consistent with the dependence on  $R$  of the breakdown time predicted by (34).

In all simulations we observed that  $\eta$  values are typ-

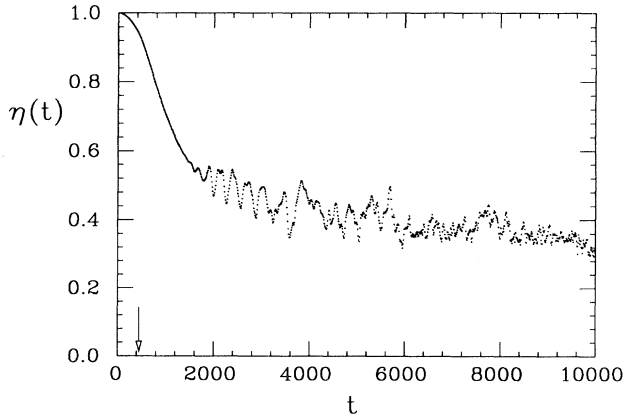


FIG. 6. Time evolution of  $\eta$  for  $N = 256$ ,  $k = 1$ ,  $R = 1.2 \times 10^{-2}$ . The shock time, shown by an arrow, is  $t_B = 424$ .

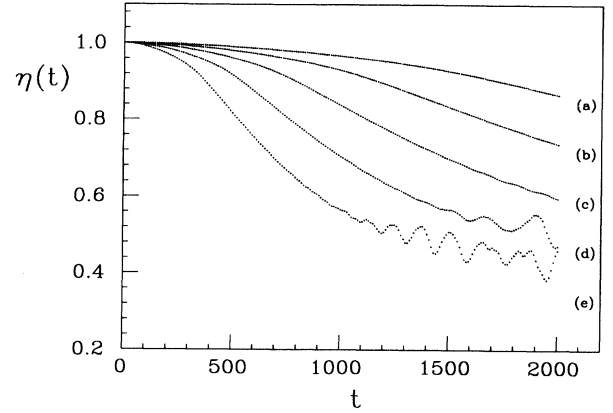


FIG. 7. Time evolution of  $\eta$  for  $N = 256$ ,  $k = 1$ , and the following values of  $R$ : (a)  $3.7 \times 10^{-3}$ ; (b)  $5.6 \times 10^{-3}$ ; (c)  $8.4 \times 10^{-3}$ ; (d)  $1.2 \times 10^{-2}$ ; (e)  $1.9 \times 10^{-2}$ .

ically slightly larger than 0.9 at the breakdown time of formula (34). This means that the shock on the lattice just begins at  $t \simeq t_B$ , thus  $t_B$  is the time at which  $\eta$  begins a sharp decay; at this time  $\eta$  has not yet decreased significantly. Indeed, the waveform, though distorted, is still close to the original one at  $t \simeq t_B$ . To relate the shock model with the temporal behavior of  $\eta$  we proceed in the following way. We fix a threshold value  $\sigma$  for  $\eta$  and we measure the time  $t_\sigma$  required for  $\eta$  to reach this threshold value (see also [19]). If  $\sigma$  is not too small, e.g.,  $\sigma \simeq 0.8-0.9$ , such a time is well defined, since  $\eta$  shows a monotone behavior decreasing below  $\sigma$ , in the range of  $R$  values explored here. Our working hypothesis is that the scaling properties of  $t_B$  with respect to the parameters  $R$ ,  $N$ , and  $k$ , expressed by (34), characterize the initial decay of  $\eta$ , then

$$t_\sigma \propto \frac{N}{kR}. \quad (35)$$

Of course the proportionality constant depends on the chosen threshold value  $\sigma$  and is not the same as in (34).

In Fig. 8 we show the dependence of  $t_\sigma$  on the number of oscillators  $N$  ( $64 \leq N \leq 1024$ ), with a fixed value of  $k$  and  $R$ . The proportionality with respect to  $N$  is well verified. We have also controlled the validity of such a property when the threshold value  $\sigma$  is changed.

Finally, we study the “universal” behavior  $t_\sigma \propto N/kR$  as a function of the single parameter  $N/kR$ . In Fig. 9 we have reported 131 experimental values of  $t_\sigma$  versus  $N/kR$ , the latter parameter spanning over approximately three decades. This was obtained varying both  $R$  (in the same interval as above) and  $N$  (from  $N = 64$  to  $N = 512$ ) and with  $k = 1$ ,  $k = 2$ , and  $k = 3$ . The predicted law is well verified and a fit of the kind

$$\log_{10} t_\sigma = a \log_{10}(N/kR) + b$$

gives  $a = 0.93$ .

An even more striking scaling law can be seen in Fig. 10, where the dependence of  $\eta$  on the rescaled time

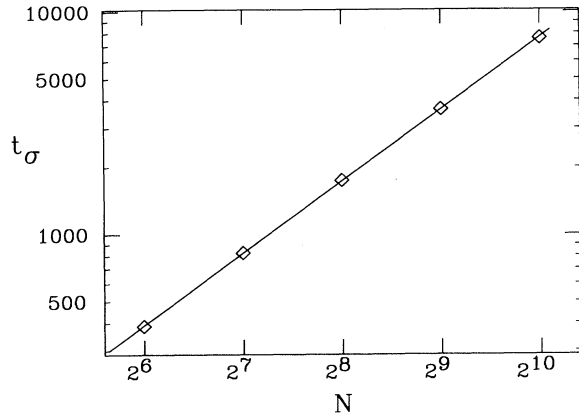


FIG. 8. Threshold time  $t_\sigma$  vs  $N$  for  $k = 1$ ,  $\sigma = 0.9$ ,  $R = 3.74 \times 10^{-3}$ . The experimental values ( $\diamond$ ) are fitted with the straight full line, whose slope, 1.07, is in agreement with the theoretical prediction of 1.

$t_R = Rt/N$  is shown for fixed  $k = 1$ , proving the independence of our results from the threshold value  $t_\sigma$ . The curves corresponding to different values of  $R$  and  $N$  collapse one on the other for  $t_R < 0.06$ .

## V. CONCLUSIONS

Our theory predicts a scaling law for the time scale characterizing the temporal evolution of the order parameter  $\eta$  in formula (2), which describes the evolution of model (3) towards equipartition of energy among Fourier modes. This prediction has been verified in numerical experiments realized in a given range of parameters ( $R, N, k$ ) and initial conditions (traveling waves). Such laws have a more general character and are valid for a larger class of initial conditions than those discussed

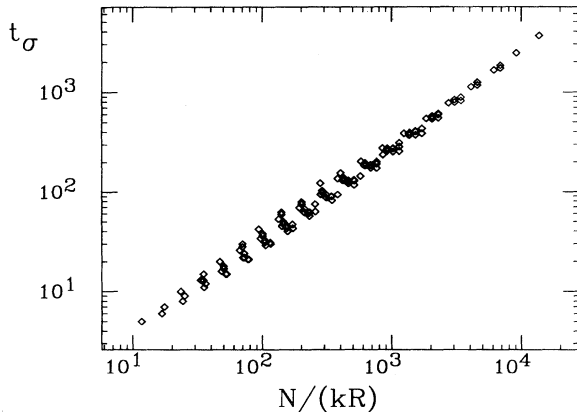


FIG. 9. Dependence of  $t_\sigma$  on the single scaling parameter  $N/(kR)$ . The plot is compatible with a slope of  $\simeq 1$ , more evident for large  $N$ .

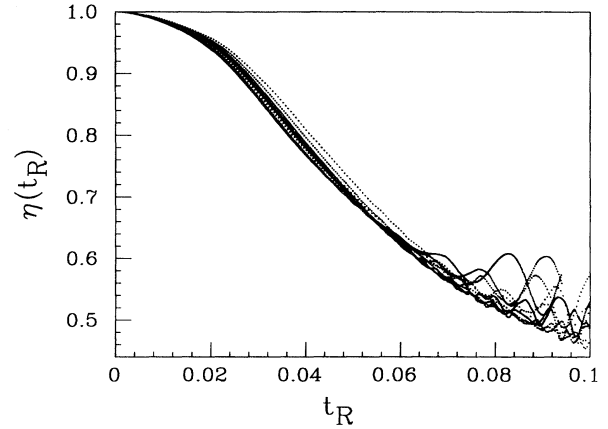


FIG. 10. Dependence of  $\eta$  on the rescaled time  $t_R = Rt/N$ . The values of  $R$  range from  $3.7 \times 10^{-3}$  to  $2.8 \times 10^{-2}$ .  $N = 256, 512$ ;  $k = 1$ . Ten different curves collapse for  $t_R < 0.06$ .

here. In fact, some very recent theoretical and numerical results [3,5,10] show a universal behavior of  $\eta$  of the kind  $\eta = \eta(\beta k E_{\text{lin}} t / N^\alpha)$  for initial conditions of a different kind (standing waves) with  $k \ll N$ . Careful numerical simulations made to clarify why in [5] and [10] two different scaling laws were found, have shown that they both are different ways to represent the universal law  $\eta = \eta(\beta k E_{\text{lin}} t / N^\alpha)$  for  $\alpha = 2$  [20]. However, the value of  $\alpha$ , predicted to be 2 also from a theory based on a low-dimensional effective Hamiltonian [10], has instead been found to be closer to 2.5 in more recent numerical simulations [3], which include in the analysis also states closer to equipartition and use as a probe a parameter  $[\exp(S)/N]$  which allows a better characterization of these states.

Moreover, a relaxation time to equipartition increasing with  $N$  has been found numerically in Ref. [21] for  $E \propto N$  and larger, looking directly at the properties of the power spectrum.

The  $\eta$  scaling law can be explained also by our theory based on shock waves. Indeed, let us consider the temporal evolution of  $\eta$  as governed by a universal law of the kind  $\eta = \eta(t/\tau)$ , where  $\tau$  is an internal time scale of the system arising from the global nonlinear interaction among its constituents and depending on the relevant parameters of the system. In the particular situation we are studying, the role of  $\tau$  is clearly played by  $t_B$ . If we suppose a scaling law for  $\tau$  of the form (34) and use (32), we find the same scaling law for  $\eta$  with  $\alpha = 2$ . The discrepancy with the most recent findings that  $\alpha = 2.5$  is seemingly due to the fact that our theory describes only the beginning of the relaxation process to equipartition, before some sizeable energy is transferred to high modes. In Ref. [3] the  $\sqrt{N}$  correction has in fact been heuristically attributed to a mode space-filling diffusive phenomenon. A modification of our continuum theory along these lines would require one to take into account the growth of small wavelength instabilities whose envelope obeys the nonlinear Schrödinger equation [22], and also the coupling of these instabilities with Eq. (15).

## ACKNOWLEDGMENTS

We acknowledge useful discussions with Carlo Alabiso, Mario Casartelli, Jayme de Luca, Allan Lichtenberg, and Roberto Livi. CINECA is acknowledged for providing CPU time on the Cray-YMP under Grant No.

G4WFIZQ1. P.P. thanks CIES and EC for financial support for his stay in Paris and the Centre E. Borel of the Institut Henri Poincaré for hospitality. We also acknowledge financial support from the European HCM Network CHRX-CT94-0546 on space-time chaos, coordinated by the Institute for Scientific Interchange in Torino, Italy.

- 
- [1] E. Fermi, J. Pasta, and S. Ulam, Los Alamos Report LA-1940 (1955) (unpublished); in *Collected Papers of Enrico Fermi*, edited by E. Segré (University of Chicago Press, Chicago, 1965), Vol. 2, p. 978.
  - [2] R. Livi, M. Pettini, S. Ruffo, M. Sparpaglione, and A. Vulpiani, Phys. Rev. A **31**, 1039 (1985); R. Livi, M. Pettini, S. Ruffo, and A. Vulpiani, *ibid.* **31**, 2740 (1985).
  - [3] J. De Luca, A.J. Lichtenberg, and S. Ruffo, Phys. Rev. E **51**, 2877 (1995).
  - [4] D.L. Shepelyansky (unpublished).
  - [5] H. Kantz, R. Livi, and S. Ruffo, J. Stat. Phys. **76**, 627 (1994).
  - [6] L. Galgani, A. Giorgilli, A. Martinoli, and S. Vanzini, Physica D **59**, 334 (1992).
  - [7] J.L. Tuck, Los Alamos Report No. LA-3990 (1968) [Adv. Math. **9**, 399 (1972)].
  - [8] N.J. Zabusky, in *Proceedings of the Conference on Mathematical Models in the Physical Sciences*, edited by S. Drobot (Prentice Hall, Englewood Cliffs, NJ, 1963), p. 99; N.J. Zabusky and M.D. Kruskal, Phys. Rev. Lett. **15**, 240 (1965).
  - [9] M. Toda, Phys. Rep. **18**, 1 (1975).
  - [10] J. De Luca, A.J. Lichtenberg, and M.A. Lieberman, Chaos **5**, 283 (1995).
  - [11] F.M. Izrailev and B.V. Chirikov, Dok. Akad. Nauk SSSR **166**, 57 (1966) [Sov. Phys. Dokl. **11**, 30 (1966)]; B.V. Chirikov, F.M. Izrailev, and V.A. Tayursky, Comp. Phys. Commun. **5**, 11 (1973).
  - [12] P. Bocchieri, A. Scotti, B. Bearzi, and A. Loinger, Phys. Rev. A **2**, 2013 (1970); M. Casartelli, G. Casati, E. Diana, L. Galgani, and A. Scotti, Theor. Math. Phys. **29**, 205 (1976).
  - [13] M. Pettini and M. Landolfi, Phys. Rev. A **41**, 768 (1990).
  - [14] L. Casetti, R. Livi, and M. Pettini, Phys. Rev. Lett. **74**, 375 (1995).
  - [15] M.J. Ablowitz and H. Segur, *Solitons and the Inverse Scattering Transform* (SIAM, Philadelphia, 1981); M.J. Ablowitz and P.A. Clarkson, *Solitons, Nonlinear Evolution Equations and Inverse Scattering* (Cambridge University Press, Cambridge, 1991).
  - [16] G.B. Whitham, *Linear and Nonlinear Waves* (Wiley-Interscience, New York, 1974).
  - [17] R. Livi, M. Pettini, S. Ruffo, M. Sparpaglione, and A. Vulpiani, Phys. Rev. A **28**, 3544 (1983).
  - [18] V.I. Arnold, *Ordinary Differential Equations* (MIT Press, Cambridge, MA, 1973), Russian original, Moscow (1971).
  - [19] H. Kantz, Physica D **39**, 322 (1989).
  - [20] H. Kantz and S. Ruffo (unpublished).
  - [21] C. Alabiso, M. Casartelli, and P. Marenzoni, Phys. Lett. A **183**, 305 (1993).
  - [22] G.P. Berman and A.R. Kolovskii, Sov. Phys. JETP **60**, 1116 (1984).